Reduction Characteristics of Carbon Dioxide Using a Plasmatron

ARTICLE *in* PLASMA CHEMISTRY AND PLASMA PROCESSING · JANUARY 2014

Impact Factor: 2.06 · DOI: 10.1007/s11090-013-9499-8

3 AUTHORS, INCLUDING:

Seong Cheon Kim

24 PUBLICATIONS **120** CITATIONS

SEE PROFILE

Young Nam Chun

Chosun University

54 PUBLICATIONS **452** CITATIONS

SEE PROFILE

Plasma Chem Plasma Process (2014) 34:125–143
DOI 10.1007/s11090-013-9499-8

ORIGINAL PAPER

Reduction Characteristics of Carbon Dioxide Using a Plasmatron

Seong Cheon Kim · Mun Sup Lim · Young Nam Chun

Received: 20 July 2013 / Accepted: 9 October 2013 / Published online: 25 October 2013

Abstract To decompose carbon dioxide, which is a representative greenhouse gas, a 3-phase gliding arc plasmatron device was designed and manufactured to examine the decomposition of CO_2, either alone or in the presence of methane with and without water vapour. The changes in the amount of carbon dioxide feed rate, the methane to carbon dioxide ratio, the steam to carbon dioxide ratio, and the methane to steam ratio were used as the parameters. The carbon dioxide conversion rate, energy decomposition efficiency (EDE), carbon monoxide and hydrogen selectivity, and produced gas concentration were also investigated. The maximum values of the carbon dioxide conversion rate, which is a key indicator of carbon dioxide decomposition, in different cases were compared. The maximum carbon dioxide conversion rate was 12.3 % when pure carbon dioxide was supplied; 34.5 % when methane was injected as a reforming additive; 7.8 % when steam was injected as a reforming additive; and 43 % when methane and steam were injected together. Therefore, this could be explained that the methane-and-steam injection showed the highest carbon dioxide decomposition, showing low EDE as 0.01 L/min W. Furthermore, the plasma produced carbon-black was compared with commercial carbon-black chemicals through Raman spectroscopy, surface area measurement and scanning electron microscopy. It was found that the carbon-black that was produced in this study has the high conductivity and large specific surface area. Our product makes it suitable for special electric materials and secondary battery materials applications.

Keywords Gliding arc plasma · Plasmatron · Greenhouse gas · Global warming · Carbon dioxide

S. C. Kim · M. S. Lim · Y. N. Chun (✉)
Department of Environmental Engineering, Chosun University, #375, Seosuk-dong, Dong-gu, Gwangju 501-759, Republic of Korea
e-mail: ynchun@chosun.ac.kr

S. C. Kim
e-mail: chuneey@gmail.com

M. S. Lim
e-mail: freshair0310@nate.com

Introduction

Carbon dioxide (CO_2) is known to be a major greenhouse gas that causes global climate changes, and is a main object of treatment because it accounts for about 80 % of all greenhouse gas emissions. With the extension of the binding obligation for CO_2 emission reduction under the Kyoto Protocol, the goal is to reduce its emission in 1990 by 25–40 % by 2020. The CO_2 is a stable conformation. A thermodynamic calculation showed that its chemical combination is broken at about 1,500 °C and that its complete decomposition into carbon (C) and oxygen (O_2) is possible beyond 5,000 °C, which indicates that much energy is needed to decompose it [1].

Most of studies on CO_2 treatment involve a carbon capture and storage (CCS) and a CO_2 reduction. The CCS is a technology that separates and captures CO_2 from places where it is produced in large volumes, compresses and transports it, and then safely stores it in ground or offshore geological storage facilities or converts it into useful materials [2]. It enables the use of fossil fuels as energy sources without great changes to existing industrial infrastructure like thermal power plants. It is becoming more important as an alternative way to achieve the CO_2 emission reduction target within the obligatory period while maintaining the existing energy supply and industrial structure based on CO_2 for the time being. It has disadvantages, however, like the danger of CO_2 leakage and the high costs of transportation and storage.

Among CO_2 reduction methods, catalytic reforming [3], electro-chemical reduction [4] and biological fixation [5] have been studied.

The catalytic reforming has been studied extensively because it can produce hydrogen (H_2) and carbon monoxide (CO), which are key elements in petrochemical engineering, through the reforming reaction of CO_2 and CH_4 using catalysts that contain metal oxides like iron, copper palladium. This endothermic reaction consumes high energy, has the problem of catalyst deactivation by the deposited carbon and requires high regeneration rate of the catalysts original activity after the reaction.

The electro-chemical reduction, which is one of the fixation methods for a large CO_2 volume, inputs electric energy to a simple electrolytic reduction reactor and converts it to chemical resources such as formic acid, methanol and ethanol by reducing the CO_2. It has not been applied yet, however, and the system has not been effectively scaled up due to the significant effects of the metal electrodes, electrolyte composition, and temperature as well as various problems such as with the electricity supply.

The biological fixation fixates the CO_2 with organic matter such as microorganisms or microalgae. This method has the disadvantages, however, of the slow growth of the microorganisms and microalgae, the unstable microalgae biomass and species, and the large space needed to remove large CO_2 volumes.

Along with these studies, studies on the application of plasma are being spotlighted as related to CO_2 decomposition. Attempts are being made to use various plasma methods to decompose CO_2, like radio frequency plasma discharge [6], corona discharge [7], dielectric barrier discharge (DBD) [8], glow discharge [9] and plasma arc discharge [10]. Studies that used the aforementioned plasma techniques achieved high CO_2 conversion rates but had low energy efficiency caused by small flow range.

Among the plasma arc discharge techniques, the gliding arc plasma discharge injects gas between electrodes at a high velocity to periodically form an arc discharge between the electrodes. It has both high and low temperature plasma characteristics [11–13]. Due to these characteristics, this technique can be used to decompose CO_2 with a high bond energy level or nondegradable harmful substances. The 3-phase alternating-current (AC)

gliding arc plasma that was used in this study is known to have higher energy decomposition efficiency (EDE) and a lower manufacturing cost, with its 3-phase power supply, than the single-phase direct-current gliding arc plasma [14].

Therefore, in this study, the 3-phase AC gliding arc plasmatron [15, 16] was used to investigate the CO_2 decomposition characteristics. The CO_2 conversion rate and EDE were investigated in a case wherein only CO_2 was supplied and in another case wherein methane and steam were added as reforming additives to improve the CO_2 decomposition effect.

Experimental System and Method

Experimental System

Figure 1 shows the plasmatron experimental system that was used to test the CO_2 decomposition characteristics. This experimental system consisted of a gliding arc plasmatron, a gas and steam feeding line, control and monitoring instruments, a measurement and analysis line, and a power supply equipment.

The gliding arc plasmatron had electrodes, an injection nozzle and a supporter. Blade-shaped electrodes (2 mm wide, 95 mm high, and 2 mm thick) were arranged at 120° with a gap of 3 mm between the electrodes fixed on a support inside the reactor. The support was made of ceramic (Al_2O_3, wt. 96 %) to insulate it from the electrodes. The outer shell of the reactor was made of a quartz tube (55 mm diameter and 200 mm long) for the observation of the plasma discharge and its insulation from the electrodes. The gas injection nozzle (3 mm diameter) was at the center of the electrode top and was fixed on the supporter [13, 14].

The gas and steam feeding lines were divided into the gas feed part (CO_2 and CH_4) and the steam feed part. The gas feed part consisted of CO_2 and CH_4 cylinders, and a mixing tank for mixing these two gases. The flow rates of these two gases were controlled by the

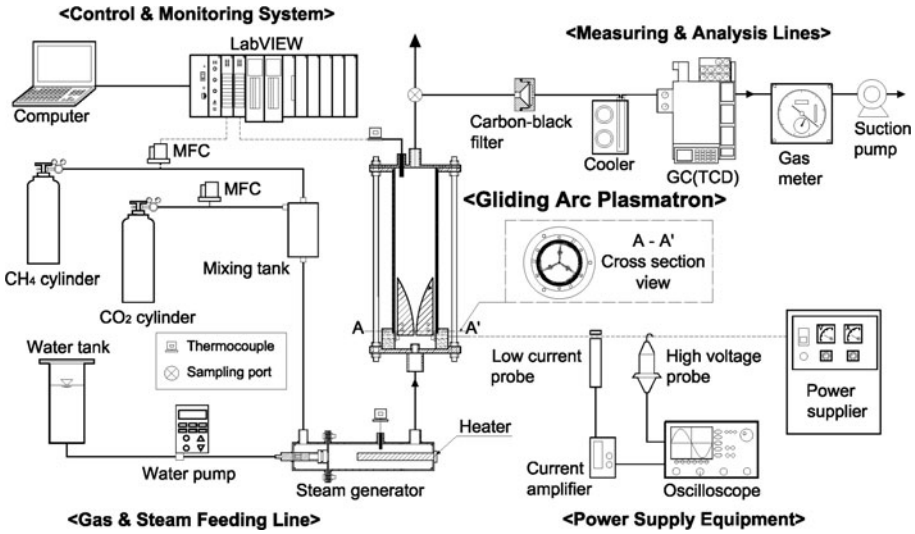

Fig. 1 Schematic diagram of the experimental system

mass flow controller (MFC). For the steam supply, water was fed by a water pump (Model STEPDOS 03, KNF, Switzerland) from the water tank to the steam generator that was kept at 400 °C. This steam was used for the steam reforming and was supplied to the plasmatron by the aforementioned the mixed gas.

For the control and monitoring instrument, LabVIEW (Model LabVIEW 8.6, National Instrument, USA) was used. It was connected to the MFC for the gas flow control; to the water pump for the water supply; and to the heater for steam generation to control the temperature of the water. These values and the temperature inside the reactor were continuously monitored.

The measurement and analysis line consisted of a carbon-black filter (Model LS-25, Advantec, Japan) for carbon-black sampling, a cooler (Model EDP 20-2, M&C, Germany) for water condensation, a gas meter (Model DC-2A, Sinagawa, Japan) and a suction pump (Model N-820.3FT 18, KNF, Switzerland). GC-TCD (Model CP-4900, Varian, the Netherlands) was used for real-time analysis of the gases.

The power supply equipment consisted of a power supply (Model UAP-15K1A, Unicon Tech., Rep. of Korea), a high-voltage probe (Model P6015, Tektronix, USA), a current probe (Model A6303, Tektronix, USA), a current amplifier (Model TM502A, Tektronix, USA) and an oscilloscope (Model TDS-3052, Tektronix, USA) for measuring the electric characteristics. The power supply could supply a 3-phase AC of up to 15 kW (voltage: 15 kV and current: 1 A) to the plasmatron.

Experiment and Analysis Method

For the experiment on the CO_2 decomposition characteristics using the plasmatron, parametric experiments were conducted for four cases, as shown in Table 1. For Case 1, the supplied flow of pure CO_2 was changed to investigate the only CO_2 decomposition characteristics. For Case 2, the CH_4/CO_2 ratio was changed to investigate the decomposition characteristics according to the changed amount of the CH_4. For Case 3, the H_2O/CO_2 ratio was changed to investigate the decomposition characteristics according to the changed amount of the steam. For Case 4, the CH_4/H_2O ratio was changed to investigate the decomposition characteristics according to the changed amount of the CH_4 and steam.

References 1 and 2 are the conditions for the comparison and analysis of the experiment results at the maximum CO_2 decomposition efficiency in Cases 2 and 4, respectively.

All the previously described experiments were conducted with the constant plasma input power of 0.6 kW.

The gases produced by the decomposition and conversion reaction of the CO_2 and the reforming additives (CH_4 and H_2O) were H_2, CO, O_2, N_2 CO_2, CH_4, C_2H_4, C_2H_6 and C_3H_8. For the CH_4 cylinder filling gas, the CNG gas for commercial vehicles was used. The filling gas was composed of CH_4 (88.9 %), C_2H_6 (8.9 %), C_3H_8 (1.3 %) and other gases (0.9 %).

Samples of produced gases were sent from the sampling port to the gas analyzer at the constant sample flow rate of 1 L/min with a suction pump. To analyze them with a dry basis, they were passed through a cooler to remove their moisture. A gas chromatograph was used for the gas analysis. CO_2, C_2H_4, C_2H_6 and C_3H_8 were analyzed with the Pora-PLOT Q capillary column (Model PPQ, Varian, the Netherlands), and H_2, CO, O_2, N_2 and CH_4 were analyzed with the Molecular Sieve 5A capillary column (Model MS 5A, Varian, the Netherlands).

The carbon-black was sampled with a suction pump for 15 min at the rate of 1 L/min, and the cumulative gas volume was measured from the gas meter. The captured carbon-black

Table 1 Conditions and ranges of the experiment parameters

Experiment	Parameter	Experiment condition (reactor temperature)	Remarks
Case 1	CO_2 supply	6–32 L/min (532–290 °C)	Only CO_2 was supplied.
Case 2	CH_4 to CO_2 ratio	0.04–1.8 (487–408 °C) (CH_4 supply: 0.5–9 L/min and CO_2 supply: 13.5–5 L/min)	Total fixed volume ($CO_2 + CH_4$) = 14 L/min
Case 3	H_2O to CO_2 ratio	0.04–0.22 (495–587 °C) (H_2O supply: 0.5–2.5 L/min and CO_2 supply: 13.5–11.5 L/min)	Total fixed volume ($CO_2 + H_2O$) = 14 L/min
Case 4	CH_4 to H_2O ratio ($CH_4 + H_2O$)/CO_2 = 1 fixed	0.99–13.18 (502–444 °C) (CH_4 supply: 3.5–6.5 L/min and H_2O supply: 3.5–0.5 L/min, CO_2 = 7 L/min)	Total fixed volume ($CO_2 + CH_4 + H_2O$) = 14 L/min CH_4 to H_2O ratio changed CO_2 supply fixed
Ref. 1	CO_2 and CH_4 experiment CH_4/CO_2 = 0.65	CO_2 = 8.4 L/min and CH_4 = 5.6 L/min	CO_2 to CH_4 ratio fixed (=6:4) Optimum condition of Case 2
Ref. 2	CH_4 and H_2O experiment CH_4/H_2O = 13.18	CH_4 = 6.5 L/min and H_2O = 0.5 L/min	CO_2 fixed (=7 L/min) Optimum condition of Case 4

(C) quantity was determined from the difference between the weights of the carbon-black filter before and after the capture. For the carbon-black filter, a glass fiber filter (Model GA-100, Advantec, Japan) that was resistant to high temperatures was used. To examine the physical and chemical characteristics of the carbon-black, that which was attached to the inner wall of the quartz tube and to the electrode surface was captured and analyzed through Raman spectroscopy (Model Ntegra, NT-MDT, Russia), specific surface area analysis (BET: Brunauer, Emmett, and Teller surface area) (Model NanoPOROSITY-XQ, MiraeSI, Rep. of Korea) and scanning electron microscopy (SEM) (Model S-4800, Hitachi Co., Japan).

Experiment Data Analysis

The performance of the gliding arc plasmatron was expressed by the CO_2 and CH_4 conversion rates, EDE, and H_2 and CO selectivities. These values were calculated with Eqs. (1)–(4), respectively.

The CO_2 or CH_4 conversion rates indicate how much of each gas is decomposed or converted to other elements. They were determined in this study as follows [17, 18]:

$$\mathrm{CR}(\%) = \frac{[\mathrm{M}]_{\mathrm{input}} - [\mathrm{M}]_{\mathrm{output}}}{[\mathrm{M}]_{\mathrm{input}}} \times 100 \tag{1}$$

wherein CR is conversion rate (%) of CO_2 and CH_4, $[M]_{input}$ is the concentrations (%) of CO_2 and CH_4, and $[M]_{output}$ is the concentrations (%) of CO_2 and CH_4.

The EDE is the amount of decomposed CO_2 against the electric energy supplied to the plasmatron. It was determined as follows [1]:

$$\mathrm{EDE}\,(\mathrm{L/min\,W}) = \frac{[\mathrm{CO_2}]_{\mathrm{CP}}}{\mathrm{IEP}} \tag{2}$$

wherein $[CO_2]_{cp}$ is the converted CO_2 flow rate (L/min) and IEP is the supplied electric power (W).

The CO selectivity is the mole concentration of CO in the product gas against the CO mole concentration in the converted gas. It was determined as follows [17, 18]:

$$\text{CO selectivity}(\%) = \frac{[CO]_{pg}}{[CH_4]_{cp} + [CO_2]_{cp}} \times 100 \quad (3)$$

wherein $[CO]_{pg}$ is the mole concentration of the CO in the product gas, $[CH_4]_{cp}$ is the mole concentration of the converted methane, and $[CO_2]_{cp}$ the mole concentration of the converted carbon dioxide.

The H_2 selectivity is the mole concentration of H_2 in the product gas against the H_2 mole concentration in the converted gas. It was determined as follows [17, 18]:

$$H_2 \text{ selectivity } (\%) = \frac{[H_2]_{pg}}{2[CH_4]_{cp} + [H_2O]_{cp}} \times 100 \quad (4)$$

wherein $[H_2]_{pg}$ is the mole concentration of the H_2 in the product gas, $[CH_4]_{cp}$ is the mole concentration of the converted methane, and $[H_2O]_{cp}$ the mole concentration of the converted steam. The volume of this steam is assumed to be identical to the injected volume.

CO_2 Decomposition Mechanism Via Plasma Discharge

The main reaction mechanisms for CO_2 decomposition and conversion by plasma arc discharge are described as follows.

Pure CO_2 Decomposition and Production Reaction [1]

In case only CO_2 is supplied in the plasmatron, it is decomposed by the electrons in the plasma reaction field to produce CO and O_2 [see Eqs. (5), (6)]. Chemical species with high energy and ions (O^+, $O_2{}^+$ and CO^+) are also produced.

Furthermore, O_2 or O_2 ions and radicals, which are reaction products in the plasma discharge, inversely react with C or CO and are reduced to CO_2 [see Eqs. (7)–(10)].

$$CO_2 + e \rightarrow CO + O + e \quad (5)$$

$$CO_2 + e \rightarrow C^+ + O_2 + 2e \quad (6)$$

$$C + (O_2)^* \rightarrow CO_2 \quad (7)$$

$$C + \left(O_2^-\right)^* \rightarrow CO_2 + e \quad (8)$$

$$C + \left(O_2^+\right)^* + e \rightarrow CO_2 \quad (9)$$

$$CO + O^* \rightarrow CO_2 \quad (10)$$

Reforming Decomposition Reaction of CO_2 and CH_4

In case methane is injected as a reforming additive into the plasmatron in which CO_2 is decomposed, in addition to the aforementioned reactions, the following representative reactions, as expressed in Eqs. (11)–(15), occur.

Methane reforming reaction [19]

$$CO_2 + CH_4 \rightarrow 2CO + 2H_2, \quad \Delta H = +247 \text{ kJ/mol} \tag{11}$$

$$CH_4 + O^* \rightarrow CO + 2H_2 + * \tag{12}$$

CO disproportionation reaction [20, 21]

$$2CO \rightarrow C + CO_2, \quad \Delta H = -173 \text{ kJ/mol} \tag{13}$$

Methane cracking reaction [18]

$$CH_4 \rightarrow C + 2H_2, \quad \Delta H = +75.2 \text{ kJ/mol} \tag{14}$$

Methane partial oxidation reforming reaction [22]

$$CH_4 + 1/2O_2 \rightarrow CO + 2H_2, \quad \Delta H = -22.6 \text{ kJ/mol} \tag{15}$$

Reforming Reaction of CO_2 and H_2O

In case steam is injected as a reforming additive, the following representative reactions occur, as expressed in Eqs. (16)–(20).

Steam decomposition reaction [23]

$$H_2O + e^- \rightarrow OH^* + H + 2e^- \tag{16}$$

$$H_2O + e^- \rightarrow 2H + O + e^- \tag{17}$$

Steam reforming reaction [24]

$$CH_4 + H_2O \leftrightarrow CO + 3H_2, \quad \Delta H = +206 \text{ kJ/mol} \tag{18}$$

CO shift reaction [25]

$$CO + H_2O \leftrightarrow CO_2 + H_2, \quad \Delta H = -41 \text{ kJ/mol} \tag{19}$$

Carbon-black oxidation reaction [25]

$$C + H_2O \rightarrow H_2 + CO, \quad \Delta H = +131 \text{ kJ/mol} \tag{20}$$

Results and Discussion

Decomposition Characteristics of the CO_2 and the Reforming Additives

To examine the CO_2 reduction characteristics of the gliding arc plasmatron, experiments were conducted to determine the parameters that would influence the CO_2 decomposition

and conversion (see Table 1). The CO_2 reduction characteristics were examined when only CO_2 was supplied and decomposed, when CH_4 or H_2O were added as a reforming additive, and when methane and steam were added simultaneously.

Decomposition Characteristics of Pure CO_2

Figure 2 shows the experiment results according to changed CO_2 injection flow at the fixed plasma input power of 0.6 kW.

Figure 2a shows the CO_2 conversion rate and the EDE. The CO_2 conversion rate gradually increased with an increase of the CO_2 injection flow, peaked to 12.3 % at 14 L/m and then decreased. This is because the plasma discharge column between three electrodes enlarged with the increase of the amount of gas inflow so that the electrons, radicals and ions increased, showing higher CO_2 decomposition. The electrons contributed especially much to the CO_2 decomposition, as shown in Eqs. (5) and (6) [26]. After having the peak value, the conversion rate decreased as the retention time of CO_2 in the plasma discharge area decreased.

The pattern of the EDE was similar to that of the CO_2 conversion rate having the peak, but the peak slightly shifted to right side. The reason is that the converted CO_2 flow rate in Eq. (2) shows the different to the difference between the input and output concentrations of CO_2 in Eq. (1); and the difference increased for the higher CO_2 feed rate.

Figure 2b shows the energy efficiency and the CO selectivity. CO and O_2 were the gases produced by the CO_2 decomposition. The concentration of the CO_2 that was not decomposed was also shown. Near the maximum decomposition of the CO_2, the CO_2 concentration was the lowest value, and the CO and O_2 concentrations were the highest. This is because as predicted, CO and O_2 are produced as CO_2 is decomposed by electrons in the plasma reaction field [see Eqs. (5), (6)]. This can also be seen in the CO selectivity, which indicates the concentration of CO among the converted CO_2 gas.

Effects of the Methane Reforming Additive on the CO_2 Destruction

Figure 3 shows the case wherein CH_4 was fed as a reforming additive for the CO_2 decomposition. The ratio of the two gas volumes was changed and the total gas supply was fixed. With the total gas flow rate and power supply fixed at 14 L/min and 0.6 kW, respectively, the CH_4 to CO_2 ratio changed from 0.04 to 1.8.

The CO_2 conversion rate increased with the CH_4 to CO_2 ratio, peaked to 34.5 % at a CH_4 to CO_2 ratio of 0.65, and decreased beyond this value. This pattern is similar to that when pure CO_2 was supplied, but the CO_2 conversion rate was higher. This is because the oxygen, which is involved in the CO_2 regeneration [Eq. (10)] by the oxidation of the produced CO, was preferably consumed in the reforming reaction of the partial oxidation of CH_4 [Eq. (15)], and this gives limitation of the CO_2 regeneration. In other words, when CH_4 is supplied as a reforming additive, the optimum CH_4 to CO_2 ratio for CO_2 decomposition is reached, showing that the CO_2 decomposition is better than that of the CO_2 supply only.

The CH_4 conversion rate gradually decreased from 73.7 % at the CH_4 to CO_2 ratio of 0.05–20.1 % at the ratio of 1.8. This is because in the case of the CH_4 conversion rate, as the CH_4 volume increases, its contribution to the CH_4 reforming reaction [Eq. (11)] decreases.

The EDE showed a pattern similar to that of the CO_2 conversion rate because both are connected to amount of CO_2 conversion. The maximum value for DRE is 0.0113 L/min W at the CH_4 to CO_2 ratio of 0.65.

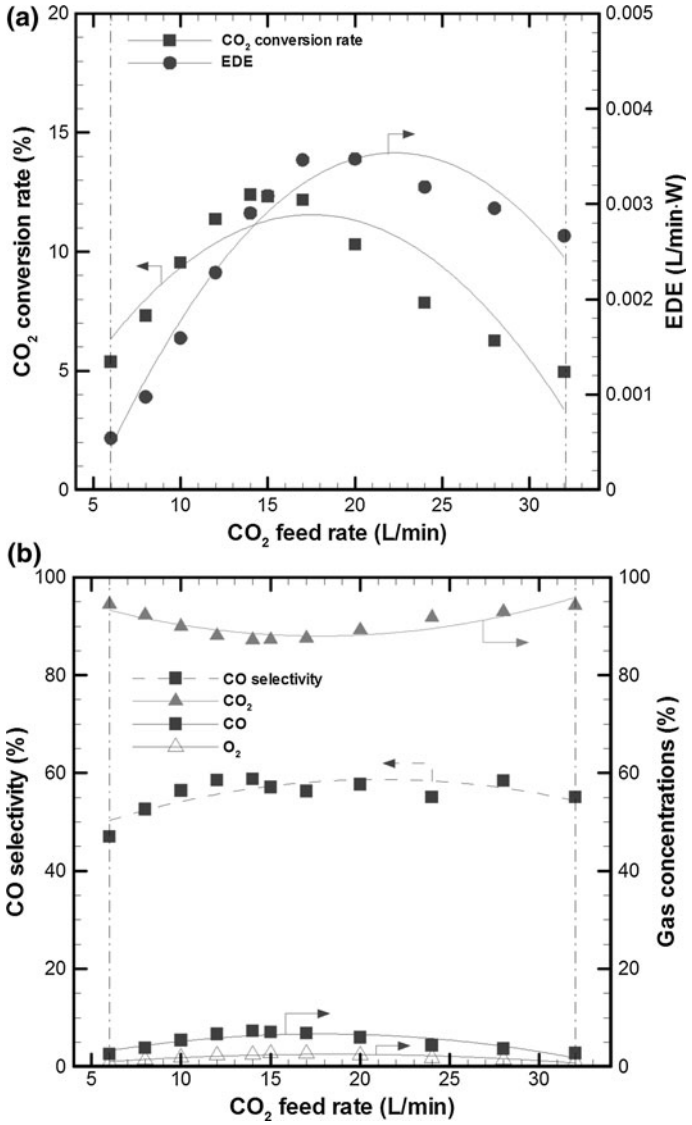

Fig. 2 Effect of the CO_2 decomposition according to the CO_2 injection feed rate. **a** CO_2 conversion rate and EDE; **b** CO selectivity and gas concentrations

The CO selectivity rapidly decreased as the CH_4 to CO_2 ratio increased because the CO_2 volume in the injection gas decreased, which also decreased the CO_2 decomposition reaction of the electrons [Eq. (5)]. The H_2 conversion rate increased with the CH_4 to CO_2 ratio, peaked to 66.2 % at a CH_4 to CO_2 ratio of 1 and then decreased. This is because as the CH_4 volume increased, the H_2 volume also increased due to the CH_4 reforming reaction [Eq. (11)] and the CH_4 cracking reaction [Eq. (14)]; but at the CH_4 to CO_2 ratio of more than 1, as the volume of the unreacted CH_4 increased, the CH_2 cracking reaction decreased due to lower retention time, which also decreased the volume of the produced H_2. The H_2

to CO ratio increased with the CH_4 to CO_2 ratio because as the CH_4 supply that contributed to the H_2 production exceeded the CO_2 supply, the H_2 conversion volume increased.

For the CO_2 and CH_4, which were the supply gases, as the CH_4/CO_2 ratio increased, the CO_2 was decomposed and its residual volume decreased, whereas the CH_4 was not fully converted and its volume gradually increased. The mostly produced gases were H_2 and CO, the values of which peaked at their respective optimum conditions for decomposition. In the case of the CO, as shown in the O_2 concentration, some of it was recombined into CO_2 through oxidation with O_2 [Eq. (10)].

The Fig. 3d represents the carbon-black and products of the hydrocarbons (C_2H_6 and C_3H_8) in the CH_4 cylinder. The C_2H_6 and C_3H_8 increased with the CH_4 to CO_2 ratio because the volume of the converted residual hydrocarbon increased. The C_2H_4 volume also increased because it was produced by the reactions expressed in the following Eqs. (21) and (22) [27].

$$2CH_4 + CO_2 \rightarrow CO + C_2H_6 + H_2O \tag{21}$$

$$C_2H_6 + CO_2 \rightarrow CO + C_2H_4 + H_2O \tag{22}$$

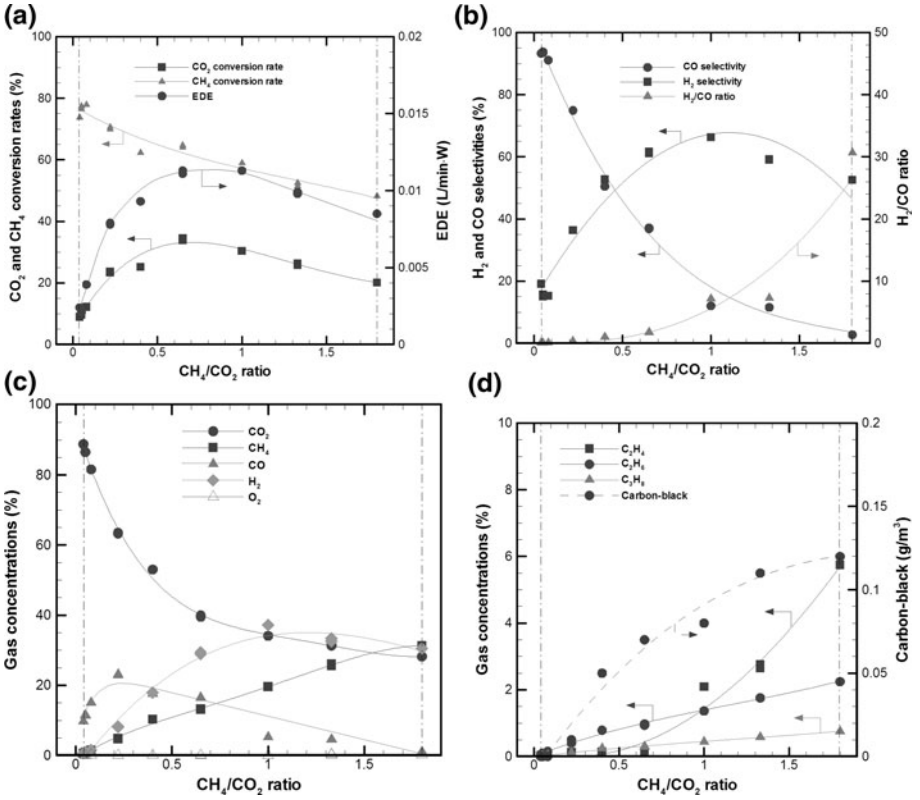

Fig. 3 Effects of the methane reforming additive on the CO_2 decomposition. **a** Conversion rates and EDE; **b** selectivities and H_2 to CO ratio; **c** concentrations of the product gases; **d** concentrations of the hydrocarbons and the carbon-black

The carbon-black increased with the CH_4 to CO_2 ratio because the carbon-black increased due to the CH_4 cracking reaction [Eq. (14)] as the amount of the injected CH_4 increased.

Effects of the Steam Reforming Additive on the CO_2 Destruction

Figure 4 shows the results of the experiment according to the change in the H_2O to CO_2 ratio to identify the effects of steam on the CO_2 decomposition, wherein the total injection flow rate and the electric input power were fixed at 14 L/min and 0.6 kW, respectively.

Figure 4a shows the CO_2 conversion rate and the EDE. The CO_2 conversion rate significantly decreased from 7.8 % at the H_2O to CO_2 ratio of 0.037–1.9 % at the ratio of 0.21. Steam makes the plasma state unstable, so the instability of the plasma discharge increased with the increase in the steam injection volume. It is more difficult for excited steam than for CO_2 to maintain its energy for a long time. Furthermore, when the steam is vibrationally-excited with CO_2, the supplied energy quickly dissipates. Moreover, steam produces an inverse reaction like the CO shift reaction [Eq. (19)] [28]. Therefore, the steam itself does not significantly affect for the CO_2 decomposition, as shown by the smaller conversion rate than pure CO_2 supply.

The energy decomposition rate decreased from 0.0018 to 0.0004 L/min W within the experimental range as the H_2O to CO_2 ratio increased. This is because the CO_2 conversion rate decreased as the amount of steam injection increased.

Figure 4b shows the CO selectivity and the gas concentrations. The CO selectivity decreased as the H_2O to CO_2 ratio increased, because the CO concentration decreased due to the CO shift reaction [Eq. (19)]. Furthermore, the amount of the product gas (CO_2, CO and O_2) decreased as the H_2O to CO_2 ratio increased, because as mentioned, the steam interferes with the plasma gas decomposition. The carbon-black was not produced when steam was injected, because a portion of the generated carbon might be oxidized by the carbon-black oxidation reaction [Eq. (20)].

CO_2 Destruction Characteristics of the Methane and Steam Reforming Additives

Figure 5 shows the case wherein both methane and steam were injected as reforming additives for the CO_2 decomposition. The CH_4 to H_2O ratio was changed at the fixed CO_2 supply of 7 L/min. The total gas flow rate and the power supply were fixed at 14 L/min and 0.6 kW, respectively.

Figure 5a shows the CO_2 and CH_4 conversion rates and the EDE. The CO_2 conversion rate gradually increased from 22.6 to 43.0 % within the experimental range as the CH_4 to H_2O ratio increased. This is because as the CH_4 injection volume increased, O_2 was consumed by the partial oxidation of CH_4 [Eq. (14)], which limited the CO_2 reduction by Eq. (10). In other words, CH_4 has a greater effect on the restriction of the inverse reaction [Eq. (10)] during the CO_2 decomposition than H_2O. The CH_4 conversion rate slightly decreased as the CH_4 to H_2O ratio increased. For the CH_4 conversion, the CH_4 reforming reaction [Eq. (11)] and the steam reforming reaction [Eq. (18)] occurred simultaneously, but the CH_4 reforming reaction had a higher energy enthalpy than the steam reforming reaction, and the CH_4 conversion rate further decreased as the CH_4 volume increased.

The EDE increased with the CH_4 to H_2O ratio and showed the same tendency as the CO_2 conversion rate. This is because as mentioned, the increased CH_4 injection volume restricted the CO_2 recombination and increased the CO_2 decomposition.

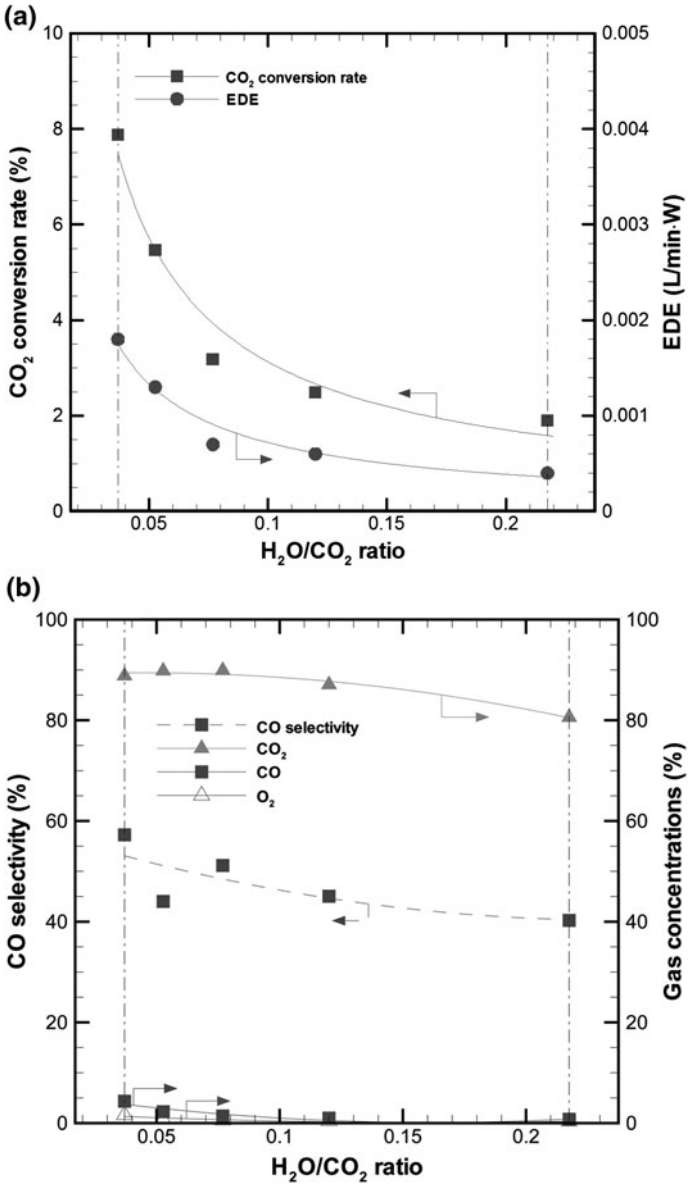

Fig. 4 Effects of the changing the amount of the steam reforming additive on the CO_2 decomposition. **a** CO_2 conversion rate and EDE; **b** selectivity and gas concentrations

Figure 5b shows the CO and H_2 selectivities and the H_2 to CO ratio. The CO selectivity significantly decreased as the CH_2 to H_2O ratio increased, whereas the H_2 selectivity gradually increased. This is because as the CH_2 volume increased, it was converted to C and H_2 by the CH_4 cracking reaction [Eq. (14)] rather than to CO by the CH_4 reforming reaction [Eq. (11)], which decreased the CO and increased the H_2. Consequently, the H_2 to CO ratio also increased with the CH_4 to H_2O ratio.

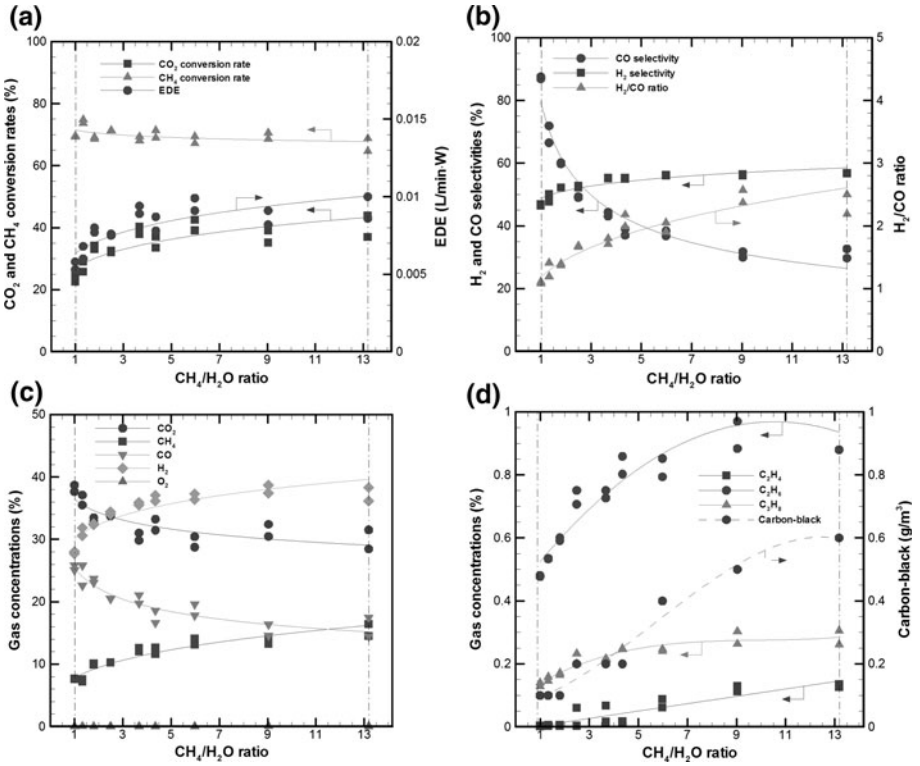

Fig. 5 Effects of the methane and steam additives on the CO_2 decomposition. **a** Conversion rates and EDE; **b** selectivities and H_2 to CO ratio; **c** concentrations of the product gases; **d** concentrations of the hydrocarbons and the carbon-black

Figure 5c shows the concentrations of the selected product gases. For the CO_2 and CH_4, which were the supply gases, as the CH_4 to CO_2 ratio increased, the CO_2 was decomposed and its amount gradually decreased due to the CH_4 reforming reaction [Eq. (11)], whereas the CH_4 was not fully converted and its amount gradually increased. The product gases that were mainly produced were CO and H_2. As the CH_4 to H_2O ratio increased, the CO gradually decreased and the H_2 increased. As the amount of steam injection decreased, the steam reforming reaction [Eq. (18)] decreased, which also decreased the CO production. Furthermore, as the amount of CH_4 injection increased, the H_2 production increased due to the CH_4 cracking reaction [Eq. (14)]. O_2 was mostly oxidized by the oxidization of carbon-black oxidization [Eq. (20)].

Figure 5d shows the concentrations of the hydrocarbon gases and the carbon-black. The hydrocarbons (C_2H_6 and C_3H_8) in the CH_4 cylinder increased with the CH_4 to H_2O ratio. The ethane (C_2H_6) increased by Eq. (21), and the destruction for the propane (C_3H_8) might decrease due to increasing the amount of the propane itself. The ethylene (C_2H_4) is a product from the Eq. (22), and also increased with increasing the amount of CH_4. Furthermore, the carbon-black increased with the CH_4 to H_2O ratio because it increased due to the CH_4 cracking reaction [Eq. (14)] as the amount of the injected CH_4 increased.

CO_2 Reduction Characteristics Under Reference Conditions

Pure CO_2 is very stable. It is decomposed by plasma discharge [Eqs. (5), (6)], but its conversion rate decreases due to the recombination reaction of the decomposed products [Eqs. (7)–(10)]. Therefore, in this study, experiments were conducted for each case (Cases 1–4) to investigate the effects of the CO_2 conversion by adding methane or steam reforming additives when CO_2 was decomposed through plasma discharge.

The results of the reference conditions in Cases 2 and 4 were compared, wherein the CO_2 conversion rate was high and carbon-black was produced. The reference conditions are referred to herein as Ref. 1 and Ref. 2 in Table 2, wherein the CO_2 decomposition is the maximum in each case.

Figure 6 shows the experiment results under these two reference conditions.

The CO_2 conversion rate (CO_2 CR in the Fig. 6) and the CH_4 conversion rate (CH_4 CR) were higher in Ref. 2, but the EDE was higher in Ref. 1. Ref. 2 showed a higher CO_2 conversion rate because the recombination of C with O_2 and its reduction to CO_2 [Eqs. (7)–(9)] were limited due to the C oxidation [Eq. (20)] by the steam additive. Ref. 2 showed a higher CH_4 conversion rate because the CH_4 was converted by the CH_4 and steam reforming reactions [Eq. (18)]. Ref. 1 showed a high EDE because in Ref. 2, the added steam made the plasma state unstable, which made the plasma discharge energy difficult continuously to maintain [1]. As a result, Ref. 2 consumed greater energy during the CO_2 decomposition. In Ref. 2, the amount of H_2 and CO are high due to the CH_4 and steam reforming reactions [Eq. (18)], but the carbon-black is small due to the carbon oxidation [Eq. (20)], as mentioned.

In addition to the aforementioned results for the two cases of Ref. 1 and Ref. 2, the physical characteristics of the plasma carbon-blacks that were produced during the CO_2 decomposition were compared with those of two commercial carbons. The commercial carbons were the carbon used for ink and tires (HS45, Orion engineered C, Rep. of Korea) and the carbon used as a conductive material for electronics (HIBLACK 420B, Orion engineered C, Rep. of Korea). These two commercial carbons were produced through pyrolysis from highly aromatic intermediate oil.

To examine the physical characteristics of carbon-blacks, Raman spectroscopy, BET analysis and SEM analysis were performed. Their results are summarized as follows.

Figure 7 shows the results of the Raman spectroscopy to compare the crystallization of plasma carbon-blacks and commercial carbons.

Graphite has one sp^2 hybridized bond layer and can be used as a conductive material because it has electric conductivity in the layer direction due to the π bond [29]. During the Raman spectroscopy, the sp^2-hybridized crystal structure, which is crystalline like graphite, shows a characteristic peak near the G-band (1,585 cm^{-1}). If there is a peak in the G-band area, the material can be regarded as having a crystallization property. From the characteristic peak of the D-band at around 1,350 cm^{-1}, the degree of the structural defect was determined [30].

For the two plasma carbon-blacks that were produced by the gliding arc plasmatron, peaks were observed at around 1,330 and 1,570 cm^{-1}. The 1,330 cm^{-1} peak generally appeared in the forms of carbon nanoparticles and the random orientation of the tubes, and the 1,570 cm^{-1} peak associated with the graphitic nature of the carbon materials [31].

As the two carbon-blacks that were sampled under the reference conditions had D-band peaks, they had the disorderly structure of the carbon layer, including the lattice defect of carbon. The carbon-blacks of the reference conditions had a higher G-band peak than the commercial carbon-black HS45, however, which shows that they had the same sp^2

Table 2 Specific surface areas of the carbon-blacks

Condition	Ref. 1	Ref. 2	HS-45	HIBLACK 420B
Specific surface area (m^2/g)	123.15	145.23	80.0	185.4

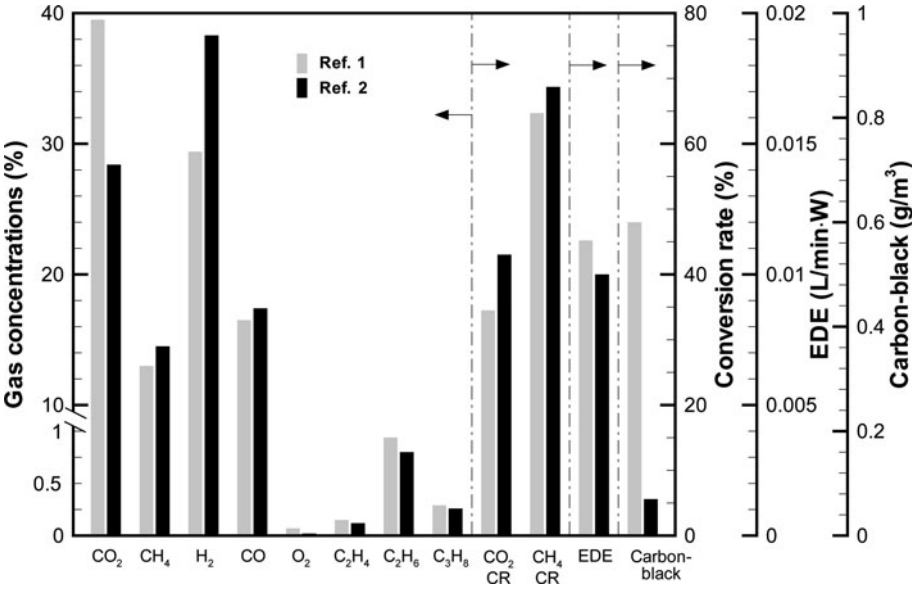

Fig. 6 Comparison of the experiment results under reference conditions

hybridized bond as graphite. Therefore, because both carbon-blacks that were produced under the reference conditions showed strong G-band areas even though such areas were weaker than those of the commercial carbon-black HIBLACK 420B, they could be used as conductive matter.

To examine the porosity of the carbon-black, its specific surface area was determined through BET analysis. The results for the reference-condition carbon-blacks and the commercial carbons are shown in Table 2.

The specific surface areas of the carbon-blacks under the reference conditions (Refs. 1 and 2) were smaller than that of the HIBLACK 420B but larger than that of the HS-45.

The two types of commercial carbons were thermal blacks created via pyrolysis, which are known to have larger specific surface areas at a higher pyrolysis temperature, as with HIBLACK 420B. The plasma black created by the plasma discharge in this study produced carbon-black through CO_2 cracking [Eq. (6)] and methane cracking [Eq. (14)]. Ref. 1, which has more stable plasma discharge with stronger energy than Ref. 2, formed more carbon-blacks. But for the specific surface area of the carbon-black, Ref. 2 was about 18 percent larger than Ref. 1. This is because some carbons in the hardened C mass were oxidized on the surface [(Eq. 20)] and micropores were formed.

Carbon-blacks that have large specific surface areas are being tested as electrode materials with the features of highly active carbon matter like intercalation compound formation, doping, and large specific surface area formation in secondary batteries and super capacitors with high energy densities [32].

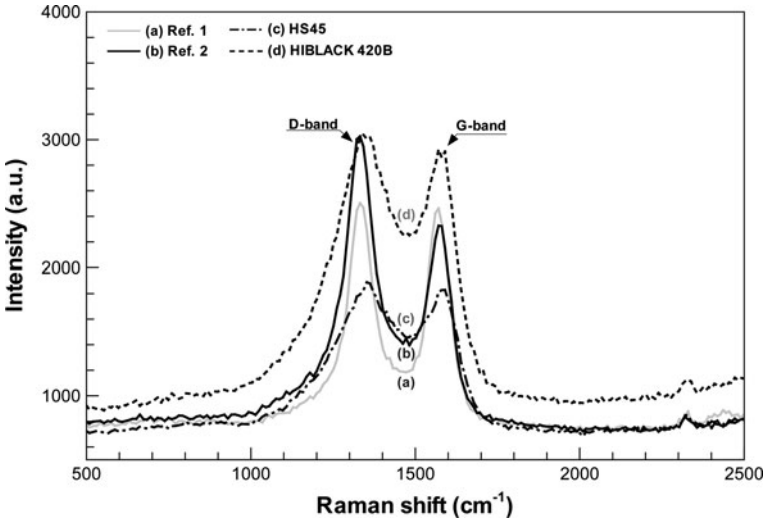

Fig. 7 Characteristics of the carbon-blacks via Raman spectroscopy

Figure 8 shows photos of the carbon-black surfaces, magnified 100,000 times under a SEM.

Carbon-blacks often exist in a collective state called a structure, which is an agglomerate combined by Van Der Waals force [33]. It has been known that the smaller the grain size of a carbon-black is, the easier it is to agglomerate. The plasma carbon-blacks [Fig. 8a, b] that were produced under the reference conditions had fine grain sizes and grew in such a way that the graphite laminates adhered to one another and formed flaky carbon-black particles shaped like wrinkled paper, but the commercial carbon-blacks [Fig. 8c, d] have differently spherical shapes.

Furthermore, both plasma carbon-blacks formed flaky carbon particles that were larger and more irregular than those of the HIBLACK 420B but smaller than those of the HS-45. These differences in shape led to the differences in the BET specific surface areas, as shown in Table 2. Although the specific surface areas of the plasma carbon-blacks were smaller than those of the HIBLACK 420B, they were larger than those of the HS-45.

CO_2 Recycling System

Figure 9 shows a CO_2 recycling system for thermal power plants based on the gliding arc plasmatron that was proposed in this study. The condition applied herein is an example of Ref. 2, wherein the greatest CO_2 reduction was attained through the simultaneous supply of methane and steam as reforming additives.

Among the gases emitted from a thermal power plant, CO_2 is separated by a membrane separator, reduced in volume to a pure CO_2 state ($CO_2 = 100$ %), and supplied to the gliding arc plasmatron. At this time, steam and hydrocarbon fuel (CH_4) are injected together as reforming additives.

CO_2 is decomposed ($CO_2 = 40$ %) from these gases by the electrochemical reaction in the plasmatron. This separated CO_2 is converted to reformed product gas ($CO_2 = 39$ %) and carbon-black ($CO_2 = 1$ %). This reformed product gas is reused as fuel for the thermal power plant. It is a high-quality gas with a high H_2 content, giving the low-pollution

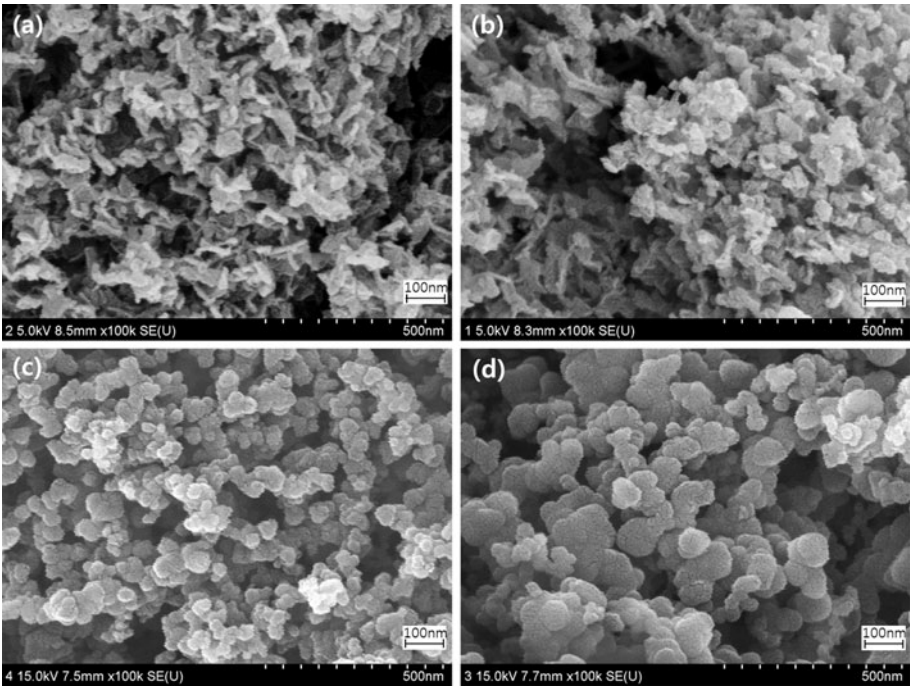

Fig. 8 Characteristics of the carbon-blacks under a SEM. **a** Ref. 1; **b** Ref. 2; **c** HS-45; **d** HIBLACK 420B

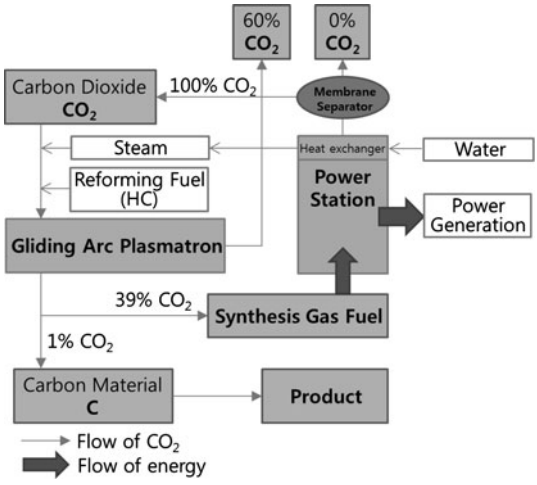

Fig. 9 CO_2 recycling system in a thermal power plant

combustion ability. Furthermore, as carbon-black has high conductivity and a large specific surface area, as mentioned, it can be used as a special electric material and a secondary battery material.

Consequently, the CO_2 recycling system should be effectively used to reduce CO_2 emissions of the fossil fuel combustion systems under the condition that there are no problems with the capacity of the plasmatron and the economically supplement of electric

power energy. The plasmatron can use the electric power from a thermal power plant, a hydroelectric power plant, a nuclear power plant, etc. For the case of the thermal power, the plasmatron contributes the greenhouse gas problem. So, the solar power and/or wind power can be used as an auxiliary energy.

Conclusion

In this study, the gliding arc plasmatron was used to decompose CO_2, which is a greenhouse gas. The CO_2 decomposition characteristics according to pure CO_2 and the addition of methane and/or steam reforming additives were also investigated.

The maximum CO_2 conversion rate was 12.3 % when pure CO_2 was supplied, 34.5 % when CH_4 was injected as a reforming additive, 7.8 % when steam was injected as a reforming additive, and 43 % when CH_4 and steam were injected together, which showed the highest CO_2 decomposition.

The injection of CH_4 to limit the recombination of the CO_2 that was decomposed by the plasma was apt for increasing the CO_2 conversion rate. Furthermore, the injection of steam oxidized the C to CO and restricted the recreation of CO_2. In conclusion, the simultaneous injection of methane and steam, which are reforming additives, effectively prevented the recombination of CO and C, which are the primary decomposed matter of CO_2.

It was found through Raman spectroscopy that the plasma carbon-blacks formed carbon with good crystallization and conductivity properties. Moreover, through BET and SEM analyses, the plasma carbon-black was found to have had an excellent specific surface area and porosity. Therefore, the carbon-blacks with excellent conductivity and porosity could be used in semiconductors and next-generation batteries.

Acknowledgments This research was supported by the Basic Science Research Program through the National Research Foundation of Korea (NRF), which is funded by the Ministry of Education, Science and Technology (No. 2012R1A1A2007144).

References

1. Indarto A, Yang DR, Choi JW, Lee H, Song HK (2007) Gliding arc plasma processing of CO_2 conversion. J Hazard Mater 146(1–2):309–315
2. Sathre R, Chester M, Cain J, Masanet E (2012) A framework for environmental assessment of CO_2 capture and storage systems. Energy 37(1):540–548
3. Jin W, Zhang C, Chang X, Fan Y, Xing W, Xu N (2008) Efficient catalytic decomposition of CO_2 to CO and O_2 over a Pd/mixed-conducting oxide catalyst in an oxygen-permeable membrane reactor. Environ Sci Technol 42(8):3064–3068
4. Hirata Y, Ando M, Matsunaga N, Sameshima S (2012) Electrochemical decomposition of CO_2 and CO gases using a porous yttria-stabilized zirconia cell. Ceram Int 38(8):6377–6387
5. Chiu SY, Kao CY, Chen CH, Kuan TC, Ong SC, Lin CS (2008) Reduction of CO_2 by high-density culture of *Chlorella* sp. in a semicontinuous photobioreactor. Bioresour Technol 99(9):3389–3396
6. Spencer L, Gallimore A (2011) Efficiency of CO_2 dissociation in a radio-frequency discharge. Plasma Chem Plasma Process 31(1):79–89
7. Wen Y, Jiang X (2001) Decomposition of CO_2 using pulsed corona discharges combined with a catalyst. Plasma Chem Plasma Process 21(4):665–678
8. Li R, Yamaguchi Y, Yin S, Tang Q, Sato T (2004) Influence of dielectric barrier materials on the behavior of dielectric barrier discharge plasma for CO_2 decomposition. Solid State Ionics 172(1–4):235–238
9. Andreev SN, Zakharov VV, Ochkin VN, Savinov SY (2004) Plasma-chemical CO_2 decomposition in a non-self-sustained discharge with a controlled electronic component of plasma. Spectrochim Acta A 60(14):3361–3369

10. Huczko A, Szymański A (1984) Thermal decomposition of carbon dioxide in an argon plasma jet. Plasma Chem Plasma Process 4(1):59–72
11. Fridman A, Nester S, Kennedy LA, Saveliev A, Mutaf-Yardimci O (1998) Gliding arc gas discharge. Prog Energy Combust Sci 25(2):211–231
12. Czernichowski A (2001) Gliding arc assisted preparation of the synthesis gas from natural and waste hydrocarbons gases. Oil Gas Sci Technol 56:181–198
13. Czernichowski P, Czernichowski A (1999) Conversion of hydrocarbons assisted by gliding electric arcs in the presence of water vapor and/or carbon dioxide. USA Patent 5,993,761
14. Lie L, Bin WB, Chi Y, Chengkang WU (2006) Characteristics of gliding arc discharge plasma. Plasma Sci Technol 8(6):653–655
15. Chun YN, Kim SC, Yoshikawa K (2012) Decomposition of benzene as a surrogate tar in a gliding arc plasma. Environ Prog Sustain Energy doi:10.1002/ep.11663
16. Chun YN, Kim SC, Yoshikawa K (2012) Removal characteristics of tar benzene using the externally oscillated plasma reformer. Chem Eng Process 57–58:65–74
17. Long H, Shang S, Tao X, Yin Y, Dai X (2008) CO_2 reforming of CH_4 by combination of cold plasma jet and Ni/γ-Al_2O_3 catalyst. Int J Hydrogen Energy 33(20):5510–5515
18. Mo LY, Fei JH, Huang CJ, Zheng XM (2003) Reforming of methane with oxygen and carbon dioxide to produce syngas over a novel Pt/$CoAl_2O_4$/Al_2O_3 catalyst. J Mol Catal A Chem 193(1–2):177–184
19. Huang A, Xia G, Wang J, Suib SL, Hayashi Y, Matsumoto H (2000) CO_2 reforming of CH_4 by atmospheric pressure ac discharge plasmas. J Catal 189(2):349–359
20. Liu BS, Au CT (2003) Carbon deposition and catalyst stability over La_2NiO_4/γ-Al_2O_3 during CO_2 reforming of methane to syngas. Appl Catal A Gen 244(1):181–195
21. Chen P, Zhang HB, Lin GD, Hong Q, Tsai KR (1997) Growth of carbon nanotubes by catalytic decomposition of CH4 or CO on a Ni MgO catalyst. Carbon 35(10–11):1495–1501
22. Li J, Lu G (2004) Reaction performance of partial oxidation of methane over Ni/SiO_2 catalysts using monodispersed silica sol as a supporting precursor. Appl Catal A Gen 273(1–2):163–170
23. Burlica R, Shih KY, Locke BR (2010) Formation of H_2 and H_2O_2 in a water-spray gliding arc non-thermal plasma reactor. Ind Eng Chem Res 49(14):6342–6349
24. Fonseca A, Assaf EM (2005) Production of hydrogen by methane steam reforming over nickel catalysts prepared from hydrotalcite precursors. J Power Sources 142(1–2):154–159
25. Elnashaie SSEH, Prasad P, Chen Z (2005) Static bifurcation characteristics of an autothermal circulating fluidized bed hydrogen generator for fuel cells. Ind Eng Chem Res 44(14):4871–4883
26. Eliasson B, Kogelschatz U (1991) Non-equilibrium volume plasma chemical processing. IEEE Trans Plasma Sci 19(6):1063–1077
27. Eliasson B, Liu CJ, Kogelschatz U (2000) Direct conversion of methane and carbon dioxide to higher hydrocarbons using catalytic dielectric-barrier discharges with zeolites. Ind Eng Chem Res 39(5):1221–1227
28. Nunnally T, Gutsol K, Rabinovich A, Fridman A, Gutsol A, Kemoun A (2011) Dissociation of CO_2 in a low-current gliding arc plasmatron. J Phys D Appl Phys 44(27):1–7
29. Reich S, Thomsen C (2004) Raman spectroscopy of graphite. Philos Trans R Soc Lond 362(1824):2271–2288
30. Dillon AC, Yudasaka M, Dresselhaus MS (2004) Employing Raman spectroscopy to qualitatively evaluate the purity of carbon single-wall nanotube materials. J Nanosci Nanotechnol 4(7):691–703
31. Saito R, Dresselhaus G, Dresselhaus MS (1998) Physical properties of carbon nanotube. Imperial College Press, London
32. Cho W, Lee SH, Ju WS, Baek YS, Lee JK (2004) Conversion of natural gas to hydrogen and carbon black by plasma and application of plasma carbon-black. Catal Today 98(4):633–638
33. Fulcheri L, Schwob Y, Flamant G (1997) Comparison of new carbon nanostructures produced by plasma with industrial carbon-black grades. J Phys III France 7(3):491–503